

# Modelling of Friction Stir Extrusion using Artificial Neural Network (ANN)

## Mohammad Ali Ansari

Department of Mechanical Engineering,  
University of Wisconsin-Madison, USA  
E-mail: aliansari1368@gmail.com

## Reza Abdi Behnagh

Faculty of Mechanical Engineering,  
Urmia University of Technology, Iran  
E-mail: r.abdibehnagh@uut.ac.ir

\*Corresponding author

## Dong Lin

Department of Industrial and Manufacturing Systems Engineering,  
Kansas State University, USA  
E-mail: dongl@ksu.edu

## Sarang Kazeminia

Faculty of Electrical Engineering,  
Urmia University of Technology, Iran  
E-mail: s.kazeminia@uut.ac.ir

**Received: 3 June 2018, Revised: 17 September 2018, Accepted: 2 December 2018**

**Abstract:** In the present study, an artificial neural network (ANN) model is developed to predict the correlation between the friction stir extrusion (FSE) parameters and the recycled wires' average grain sizes. FSE is a solid-state synthesis technique, in which machining chips are firstly loaded into the container, and then a rotating tool with a central hole is plunged into the chips at a selected rotational speed and feed rate to achieve indirect extrusion. Selecting rotational speed (RS), vertical speed (VS), and extrusion hole size (HS) as the input and average grain size as the output of the system, the 3–6–1 ANN is used to show the correlation between the input and output parameters. Checking the accuracy of the neural network, R squared value and Root-Mean-Square-Error (RMSE) of the developed model (0.94438 and 0.75794, respectively) have shown that there is a good agreement between experimental and predicted results. A sensitivity analysis has been conducted on the ANN model to determine the impact of each input parameter on the average grain size. The results showed that the rotational speed has more effect on average grain size during the FSE process in comparison to other input parameters.

**Keywords:** Average Grain Size, Artificial Neural Network, Friction Stir Extrusion, Recycling, Sensitivity Analysis

**Reference:** Ansari, M.A., Abdi Behnagh, R., Lin D., and Kazeminia, S., “Modelling of Friction Stir Extrusion using Artificial Neural Network (ANN)”, Int J of Advanced Design and Manufacturing Technology, Vol. 11/No. 4, 2018, pp. 1–12.

**Biographical notes:** **Mohammad Ali Ansari** received his MSc in Mechanical Engineering from University of Tehran. He is currently PhD student at the University of Wisconsin-Madison. **Reza Abdi Behnagh** is an assistant professor of the mechanical engineering department, Urmia University of Technology. His current research focuses on multi advanced manufacturing and simulation. **Dong Lin** is an assistant professor of Industrial and Manufacturing Systems Engineering, Kansas State University. His current research focuses on 3D printing of multifunctional aerogels for various application. **Sarang Kazeminia** is an assistant professor of the electrical engineering department, Urmia University of Technology. His current research focuses on the design and implementation of high-resolution data converters.

## 1 INTRODUCTION

Magnesium alloys are widely applied in the aerospace and automotive industries due to their unique physical and mechanical properties such as low density, high specific strength, high specific stiffness, and high thermal conductivity [1]. Since magnesium has good machinability, a high quantity of chips is available for recycling. In traditional recycling method, which is based on melting, a high percentage of materials are oxidized during the process. Therefore, solid-state recycling process is an excellent substitution for the traditional method regarding energy efficiency and material loss [2–4]. Based on previous studies [5–7], magnesium solid-state recycling can modify the mechanical properties of the material through homogeneous oxide dispersion and nucleating fine grains.

Combining direct solid-state processing and friction stir welding (FSW), friction stir extrusion (FSE) can be used to recycle the magnesium chips [8–9]. Therefore, FSE can produce a product with proper mechanical properties by converting scraps and chips into extruded bulk directly. Additionally, the FSE follows the FSW principles where a rotational tool generates frictional heating, resulting in material softening by plastic deformation [10]. Hence, the method is a potential material processing method without external heating resources that convert magnesium, aluminum, and titanium (known as lightweight materials) scraps and chips into the usable products [11–12]. Due to material movement in the scrolled face of the rotating tool, severe plastic deformation happens during extrusion.

As reported, dynamic recrystallization (DRX) results in equiaxed and fine grains during the FSE process [13–15]. Therefore, the grain size is an evaluative factor to investigate the mechanical properties of extruded wires and it is a critical element to modify the functional and structural properties of processed material such as tensile strength, or microhardness [16]. Thus, it is important to use mathematical and analytical models for better understanding of process structure and predicting the processed material properties, i.e. necessary to improve the manufacturing process and achieve a desired quality. There are two major techniques for developing mathematical models. The first method is response surface methodology (RSM) which is a linear, straightforward approximation technique, using the regression analysis and the design surface to analyse the model [17–18].

In different studies [19–22], the RSM technique has been used to develop the mathematical model and then, the analysis of variance (ANOVA) have been utilized to validate the developed model. The second method, known as the artificial neural network (ANN), is an approximation tool that is inspired by natural networks which use many neurons as computational sections for

training, validation, and test of the model [23]. Some of the work done in this area is as follows: Okuyucu et al. [23] have predicted the hardness of heat affected zone (HAZ), the hardness of weld metal, elongation, yield strength, and tensile strength of aluminum friction stir welding joints. The mean-error for the hardness of HAZ, the hardness of weld metal, elongation, yield strength, and tensile strength have been reported around 1.325, 0.656, 7.596, 3.570, and 1.650, respectively.

Asadi et al. [24] have predicted the grain size and hardness of AZ91/SiC of friction stir processing (FSP) nanocomposite plate. As calculated, the maximum training errors for the hardness and grain size are 0.5% and 1.8%, respectively. Yousif et al. [25] have developed an ANN model to predict the friction stir welding of AA6061 aluminum tensile stress, bending stress, and elongation. The errors of tensile stress, bending stress, and elongation are 1.7524 %, 7.3777 %, and 11.98 %, respectively. Ghetiya et al. [26] have used ANN with 4–8–1 architecture to predict the tensile strength of FSW joint with less than 3% error. Arunchai et al. [27] have utilized the ANN to model the Resistance Spot Welding (RSW) joints mechanical properties with the accuracy of 95%.

Comparing the accuracy, Lakshminarayanan et al. [18] have tested both RSM and ANN methods for modelling the friction stir welding of AA7039 aluminum alloy strength. The calculated Mean-error of ANN and RSM models to predict the joints tensile strength are 0.258 and 0.769, respectively. As the results show, the ANN can model the process more accurately. In addition, it has been investigated [28] that although RSM is unable to give any information about parameters' relationship, the ANN can recognize the importance of each parameter and its impact on the output of the system.

A review of the literature conducted in using ANN for modelling of similar processing techniques suggests that this method has a very high capability to optimize the FSE process. On the other hand, while there are sufficient experimental studies on experimental analysis of friction stir extrusion, the use of the ANN technique to optimize the process has not been reported so far. Also, there is no mathematical model to evaluate the effect of input parameters on the final properties of processed material during the FSE process.

In addition, because the processed material grain size is an important factor to analyse the properties of wires and there is lack of study on the average grain size of processed material, the analytical analysis is important to understand the relationship between FSE parameters. Hence, to tackle the aforementioned limitations, this paper presents a mathematical model based on ANN to analyse the FSE process of magnesium. The feed-forward neural network with the back-propagation algorithm is employed to find the correlation between FSE parameters and average grain size of the produced

wires. Root–Mean–Square–Error (RMSE) and linear regression analyses are used to show the accuracy of the developed model. Finally, the sensitivity analysis is employed to test the relative importance of input parameters on average grain size.

**2 EXPERIMENTAL STUDY**

To extrude Mg wires in the FSE process, clean and dry magnesium chips produced directly from Mg ingot and through planning machine, are used. Mg chips were clean and have an average width, length, and thickness of 1–4, 6–10, and 0.2 mm, respectively. Magnesium ingot has a coarse grain size of 1mm, distributed uniformly in the as–received material, whereas the magnesium chips have an average grain size about 14 μm which is reduced after machining process. The present chemical composition of pure Mg is (in weight percent): <0.01% Al, 0.005% Ca, 0.006% Cu, 0.005% Zn, 0.03% Mn, <0.002% Sn and balanced Mg. Two main components of experimental setup are the container and rotating tool with a scrolled face that facilitates the flow of the deformed material toward the extrusion hole. Both of components are made of tempered and quenched H13 tool steel. The dimensions of the container are 21mm and 50mm in depth while rotating tool have an outer diameter of 20 mm and extrusion hole diameter of 5mm which have scrolled face pattern at a 0–degree tilt angle. The container is fixed on the table of the modified CNC milling machine and then the die is rotated in the clockwise direction and plunged into the container that is filled with the Mg chips.

Figure 1 shows the friction stir extrusion experimental setup. During the process, magnesium chips are stirred due to the conversion of mechanical energy to thermal energy, leading to flowing the deformed material toward the central hole. Then the extrusion process is completed. For microstructural analysis of extruded wires, optical

microscopy (OM) has been used. The analyses are applied along the cross–section of wires, perpendicular to the extrusion direction. Specimens are prepared by standard metallographic techniques and etched with an Acetic–picral solution (5 ml Acetic Acid, 6 g Picric acid, 10 ml water and 100 ml ethanol) for 5 seconds at room temperature. The linear intercept technique had been used to measure average grain size for each sample.

The microstructure and grain size distribution histogram of the produced wire with the rotational speed of 250 rpm, vertical speed of 20 mm/min, and extrusion hole size of 5 mm are shown in “Fig. 2”. For all extruded wires, the OM micrographs of the microstructure are taken close to the wire center. For all of the micrographs, there is no sign of cracks or voids which is the result of grain refinement in the extruded wires. The experimental results are shown in “Table 1”. It is obvious that the average grain size for all of the specimens is varied due to a different amount of heat and deformation rate. As shown, the process input parameters are the rotational speed, vertical speed, and extrusion hole size and the output is average grain size.

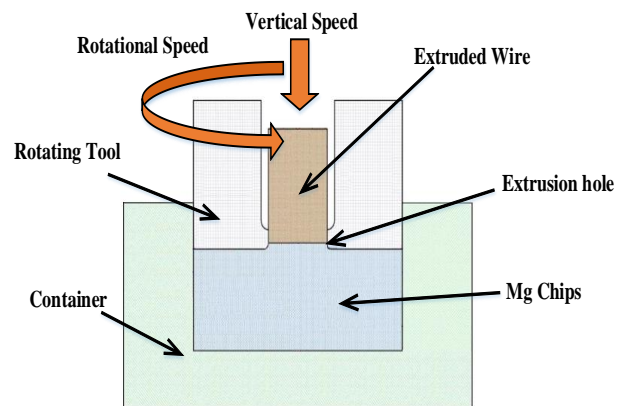


**Fig. 1** Schematic of friction stir extrusion setup.

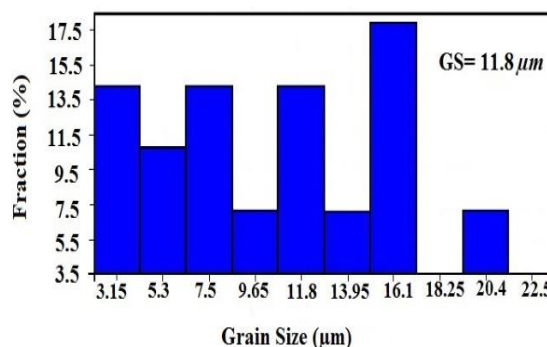
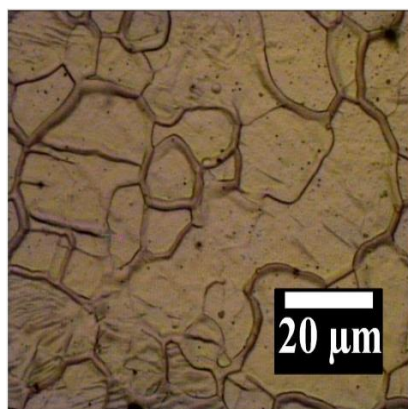


**Fig. 2** Microstructure and histogram of grain size distribution for wire with the rotational speed of 250 rpm; vertical speed of 20 mm/min, and extrusion hole size of 5 mm.

**Table 1** The experimental results

No	Input Parameters			Output
	Rotational speed (rpm)	Vertical speed (mm/min)	Hole size (mm)	Average grain size ( $\mu\text{m}$ )
1	250	14	4	8.8
2	250	14	4	8.1
3	250	14	5	10
4	250	14	5	9.4
5	250	20	4	6.1
6	250	20	4	6.7
7	250	20	5	10
8	250	20	5	11.8
9	355	14	4	14.5
10	355	14	4	11.9
11	355	14	5	15.1
12	355	14	5	15.7
13	355	20	4	12.1
14	355	20	4	13.9
15	355	20	5	13.8
16	355	20	5	15
17	180	14	4	13.1
18	180	14	4	13.8
19	180	14	5	15.9
20	180	14	5	17.8
21	180	20	4	13.9
22	180	20	4	14.8
23	180	20	5	15.4
24	180	20	5	15.6

### 3 ARTIFICIAL NEURAL NETWORK

The neural network consists of several layers that have one or more neurons, utilized as a computational tool. The principle of artificial neural network to model the process is based on four laws: (a) neurons of each layer are connected to all neurons of the next layer which is passed through special activation function, (b) weight modification between neurons is done in order to adjust the accuracy of the system, (c) we need to train the network using input patterns to determine the network topology, and (d) we can use the established model to predict the output after training is done [29]. There are

different types of feedforward neural network to model the mechanical processes. Among them, multi-layered perceptron (MLP) is the simplest neural network architectures [30]. MLPs are constructed from several parallel layers including input and output layer as the first and last layer of the network and in-between, there are one or more hidden layers.

Figure 3 shows a three-layer MLP network. When the network architecture is defined, the training step (forward and backward pass) will begin to determine the weights of the system. During the forward pass, synaptic weights are considered constant and the influence of the input parameter of the network is propagated layer by layer throughout the network. During the backward pass,

the synaptic weights modification is done via error calculation between the experimental and calculated results. This cycle will continue until the error is less than desired value [31–32]. The local minimum error of the network can be calculated through different Back Propagation (BP) algorithms including conjugate gradient method, Gauss–Newton’s method, gradient descent method, variable–metric method, and Levenberg Marquardt (LM).

Among these algorithms, the LM is the fastest one to update the weights and has the best performance [33]. Although validation step is part of training step, it is employed to guide the network performance by controlling the learning rate, deciding when it is the time to stop training, avoiding model to be overfitted, and tuning the model parameters. Finally, the trained network is examined and validated by the test step. Then, if the calculated outputs are close enough to the actual ones, the network can be used as a useful and accurate predictive tool to predict the output [31], [32].

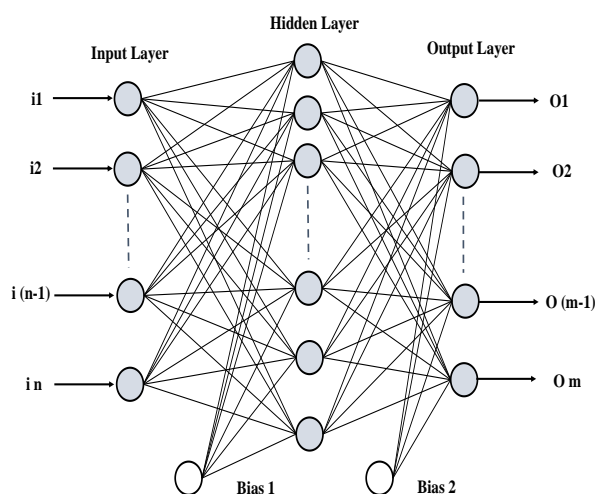


Fig. 3 A multilayered perceptron schematic.

#### 4 PROPOSED ANN MODEL

In the current study, to model the FSE process, MLP feed–forward neural network and Levenberg Marquardt backpropagation algorithm have been used to train the network [34]. The proposed ANN model takes rotational speed, vertical speed, and extrusion hole size as input parameters and average grain size as output. The dataset consists of 24 experimental data which have been normalized through whitening transformation, represented by  $x$  in the following equation:

$$\hat{x} = \frac{x - \mu}{\sigma} \tag{1}$$

Where  $x$ ,  $\mu$  and  $\sigma$  are the average and the standard deviation of each input parameter variation. With an appropriate network, different architectures including various activation function in the hidden and output layer and a different number of neurons in a hidden layer have been tested. The performance of different networks has been measured using Root–Mean–Square–Error (RMSE) (“Eq. 2”) and correlation coefficient (“Eq. 3”) between the experimental and predicted results (“Table 2”).

$$RMSE = \sqrt{\frac{\sum_{i=1}^n (y_i - \hat{y}_i)^2}{n}} \tag{2}$$

$$R \text{ squared value} = R^2 = 1 - \frac{\sum_{i=1}^n (y_i - \hat{y}_i)^2}{\sum_{i=1}^n (y_i - \bar{y}_i)^2} \tag{3}$$

Based on the table, the total RMSE and R squared values for a model with 6 neurons in a hidden layer and “tan–sigmoidal” and “linear” activation function for hidden and output layer are 0.75794 and 0.944376 which are much better results than other networks. Therefore, this architecture has been chosen as the basic network in this work. Schematic of 3–6–1 architecture is presented in “Fig. 4”. The ANN flowchart, used in this study to predict the average grain size, is shown in “Fig 5” [35]. To model the process, the “MATLAB R2017.a” [36] has been used to train, validate and test the network.

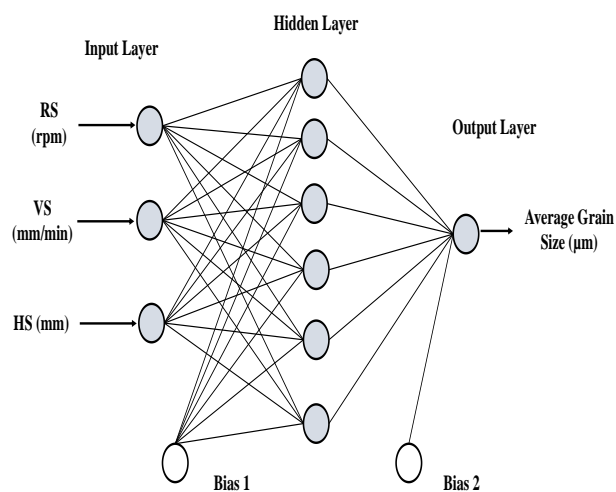


Fig. 4 Schematic of the current three–layer neural network.

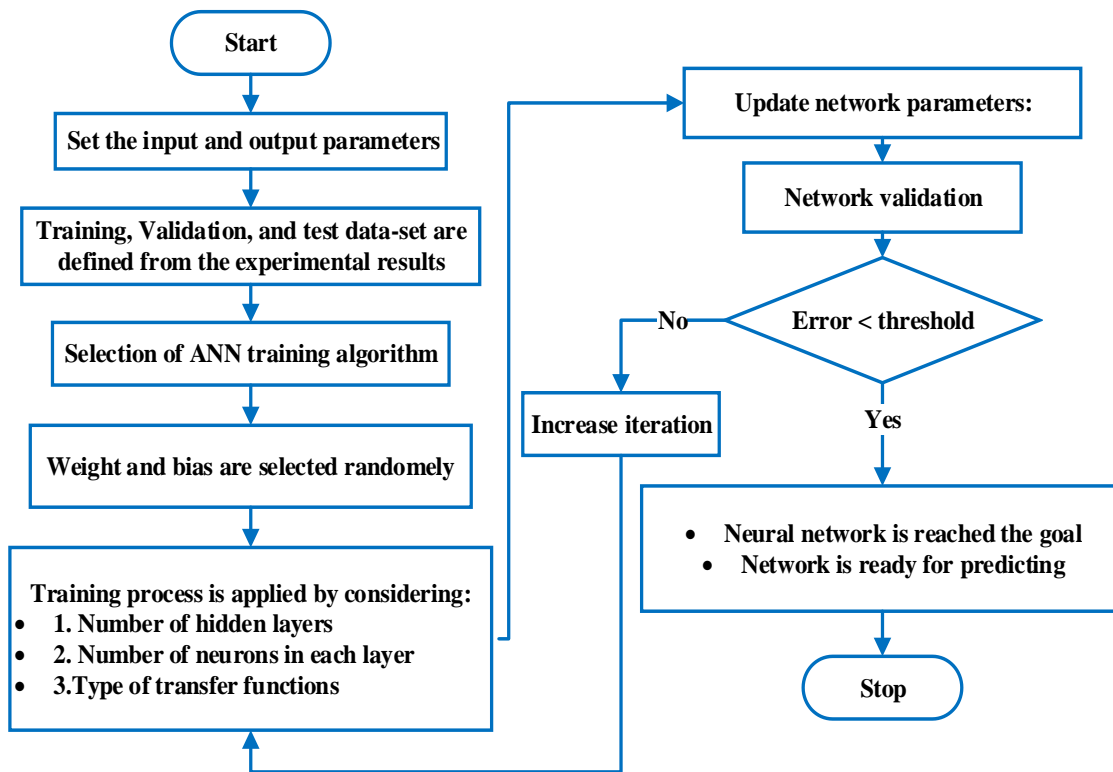


Fig. 5 The ANN model flowchart.

Table 2 Different architectures for networks and corresponding performance

No.	Activation Function		Neurons in hidden layer	Model RMSE	Model R squared value
	Hidden Layer	Output layer			
1	Tansig	Tansig	5	2.1321	0.692108
2	Tansig	Tansig	6	2.0205	0.582123
3	Tansig	Logsig	5	2.3538	0.610195
4	Tansig	Logsig	6	2.1833	0.664551
5	Tansig	Purelin	5	0.83973	0.934586
6	Tansig	Purelin	6	0.75794	0.944376
7	Logsig	Tansig	5	1.4804	0.774259
8	Logsig	Tansig	6	1.1591	0.877613
9	Logsig	Logsig	5	2.7957	0.335832
10	Logsig	Logsig	6	2.3032	0.681467
11	Logsig	Purelin	5	1.6523	0.716799
12	Logsig	Purelin	6	1.2278	0.863171

## 5 ANN RESULTS AND DISCUSSION

Using the proposed structure to model the FSE process, 14 experiments have been used for training the network and both validation and test steps have used five experiments. Figure 6a–d represents the experimental and predicted results in all steps. Furthermore, the actual and predicted values of average grain size at the training, validation, and test steps are presented in “Table 3”.

According to the “Fig. 6”, the proposed ANN can predict the output in good agreement with the experimental results. Furthermore, the Root–Mean–Square–Error at training, validation, test, and all steps together are 0.75349, 0.76796, 0.76027, and 0.75794, respectively. Regarding several studies [37–38], the RMSE smaller than 2% of the output value is an acceptable error for the network. Thus, the ANN output has a close relationship with the experimental results and can predict the average grain size precisely.

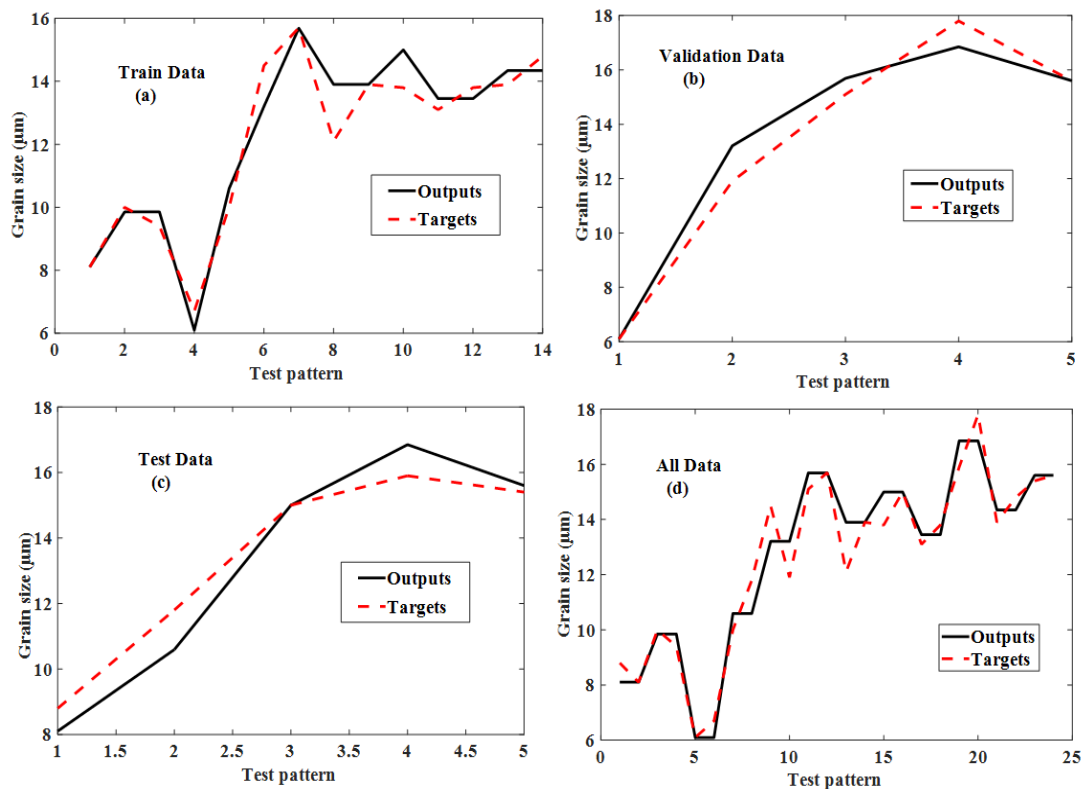


Fig. 6 The actual and predicted values of average grain size: (a): The training step, (b): Validation step, (c): Testing step and (d): All steps together.

Table 3 The actual and predicted values of grain size at the training, validation, and test steps

Stage	No.	RPM (rpm)	VS (mm/min)	HS (mm)	Average grain size (µm)		Error	Error %	RMSE
					Actual	calculated			
Training	1	250	14	4	8.1	8.102172	-0.00217	0.02681	0.75349
	2	250	14	5	10	9.850278	0.149722	1.497224	
	3	250	14	5	9.4	9.850278	-0.45028	4.790187	
	4	250	20	4	6.7	6.096957	0.603043	9.000643	
	5	250	20	5	10	10.59151	-0.59151	5.915069	
	6	355	14	4	14.5	13.20398	1.296021	8.938077	
	7	355	14	5	15.7	15.68823	0.011769	0.074964	
	8	355	20	4	12.1	13.9002	-1.8002	14.87769	
	9	355	20	4	13.9	13.9002	-0.0002	0.00144	
	10	355	20	5	13.8	14.99962	-1.19962	8.692929	
	11	180	14	4	13.1	13.44995	-0.34995	2.671357	
	12	180	14	4	13.8	13.44995	0.350052	2.53661	
	13	180	20	4	13.9	14.34518	-0.44518	3.202743	
	14	180	20	4	14.8	14.34518	0.454819	3.073099	
Validation	1	250	20	4	6.1	6.096957	0.003043	0.049887	0.76796
	2	355	14	4	11.9	13.20398	-1.30398	10.95781	
	3	355	14	5	15.1	15.68823	-0.58823	3.895567	
	4	180	14	5	17.8	16.85002	0.949977	5.336949	
	5	180	20	5	15.6	15.60019	-0.00019	0.00125	
Testing	1	250	14	4	8.8	8.102172	0.697828	7.929868	0.76027
	2	250	20	5	11.8	10.59151	1.208493	10.24147	
	3	355	20	5	15	14.99962	0.000376	0.002505	
	4	180	14	5	15.9	16.85002	-0.95002	5.974988	
	5	180	20	5	15.4	15.60019	-0.20019	1.299967	

## 6 REGRESSION ANALYSIS

Through applying linear regression analyses, the correlation coefficients ( $R^2$ ) are computed between experimental and calculated values in the developed

model. For all of three input parameters, “Fig. 7” represents the comparison between the experimental and predicted data at training, validation, test, and entire model. Because the  $R^2$  values are very close to the unit number, the proposed neural network can predict the output accurately.

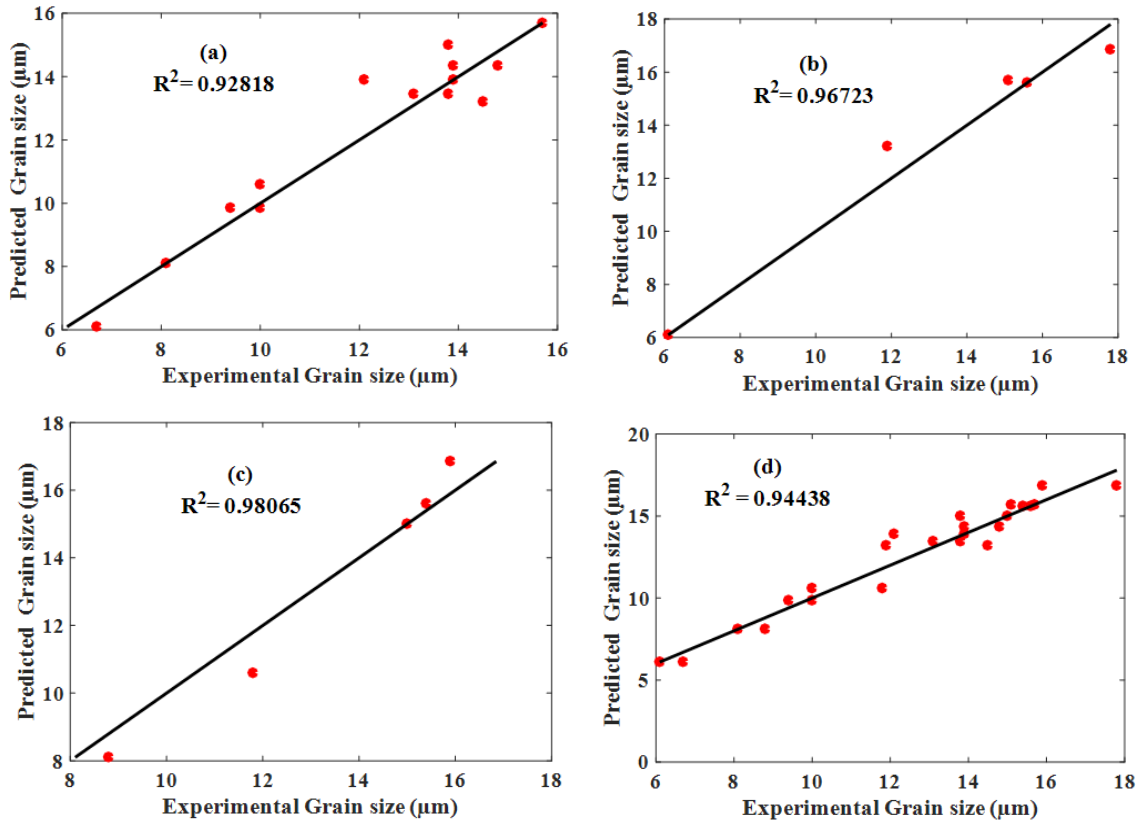


**Fig. 7** Correlation between actual and predicted data at: (a): training step, (b): validation step, (c): test step and (d): all steps together.

## 7 FORMULATION

Creating a mathematical formula to predict the average grain size, the developed neural network weights have been extracted. In the proposed network, firstly, the input layer parameters are multiplied by the hidden layer weights and then are added to hidden layer biases. The summations are passed through “tansig” (“Eq. 4”) transfer function (Eq.  $f_1 - f_6$ ). Afterward, they are multiplied by the output layer weights and added to output layer bias. Finally, they pass through “purelin” transfer function (“Eq. 5”) to generate the output (“Eq. 6”).

$$\text{tansig}(x) = \frac{2}{(1+e^{-2x})} - 1 \quad (4)$$

$$\text{purelin}(x) = x \quad (5)$$

$$\text{Average grain size} = -0.62244f_1 + 0.382324f_2 - 0.79684f_3 - 0.29625f_4 - 0.33067f_5 - 0.98962f_6 + 1.17337155 \quad (6)$$

Where  $x$  is the weighted summation of the input.

$$f_1 = \frac{2}{1+e^{-2(1.47266(\text{RS})+1.00608(\text{VS})-1.93075(\text{HS})-2.49435)}} - 1 \quad (7)$$

$$f_2 = \frac{2}{1+e^{-2(1.72452(\text{RS})+1.360273(\text{VS})+0.321748(\text{HS})-2.04292)}} - 1 \quad (8)$$

$$f_3 = \frac{2}{1+e^{-2(-2.25114(\text{RS})+0.57049(\text{VS})+0.783208(\text{HS})+1.778691)}} - 1 \quad (9)$$

$$f_4 = \frac{2}{1+e^{-2(-0.71733(RS)+0.256621(VS)-2.99931(HS)-1.428)}} - 1 \quad (10)$$

$$f_5 = \frac{2}{1+e^{-2(0.019349(RS)-1.11877(VS)+1.992122(HS)+1.908361)}} - 1 \quad (11)$$

$$f_6 = \frac{2}{1+e^{-2(2.827377(RS)+0.117701(VS)-0.04241(HS)+2.723661)}} - 1 \quad (12)$$

Where RS, VS and, HS are rotational speed, vertical speed, and extrusion hole size, respectively. It should be noted that to calculate the average grain size, all parameters in “Eqs. 7 to 12” should be normalized by whitening transformation (“Eq. 1”).

### 8 SENSITIVITY ANALYSIS AND MODEL INTERPRETAION

Sensitivity analysis has been conducted to recognize the important input parameters and its order in the developed ANN model. Hence, sensitivity analysis can present useful information about the model “robustness” which leads to having a better decision making during the process. For analysing the developed neural network structure, different methods have been suggested since the end of the 1980s. There are two main approaches: the first method is weights magnitude and the second one is sensitivity analysis [36].

### 9 WEIGHT MAGNITUDE METHOD

Weights magnitude technique is solely based procedure which analyzes the network based on the stored value in the weights matrix of the model to extract the relative importance of each input parameter. This kind of analysis is proposed by Garson through “Eq. 13” [39], where  $Q_{ik}$  defines the impact percentage of the input variable  $x_i$  on the calculated output  $y_k$ . The other input parameters contribution is calculated by considering the total amount of index which is 100% [40] (Different input parameters of the developed model relative importance is calculated in Appendix).

$$Q_{ik} = \frac{\sum_{j=1}^L \left( \left( \frac{w_{ij}}{\sum_{r=1}^N w_{rj}} \right) v_{jk} \right)}{\sum_{i=1}^N \left( \left( \frac{w_{ij}}{\sum_{j=1}^L w_{rj}} \right) v_{jk} \right)} \quad (13)$$

Where  $\sum_{r=1}^N w_{rj}$  represents the weights summation between the input and hidden layer neurons. “Table. 4” shows the relative importance of rotational speed, vertical speed, and extrusion hole size as input

parameters on average grain size. Based on the table, the effect of rotational speed, vertical speed, and extrusion hole size are 38.19387, 21.60877 and, 40.1973, respectively. Therefore, the influence of rotational speed is more than vertical speed, while the extrusion hole size has more impact than other two factor.

**Table 4** Relative importance of input parameters on average grain size

Relative importance (%)		
RS	VS	HS
38.19387	21.60877	40.19736

### 10 PAD METHOD

Using sensitivity analysis for the developed ANN model, the Pad method is usually employed [41]. In this technique, the derivative of ANN outputs is calculated concerning each input. The  $m^{th}$  output is calculated using (“Eq. 14”) for a neural network with  $n_i$  neurons in input layer,  $n_j$  neurons in the hidden layer,  $n_k$  neurons in the output layer, and “Tansig” and “Purelin” transfer function for hidden and output layer, respectively.

$$y_m = \sum_j W_{mj} \text{tansig}(\sum_i W_{ji} X_i + b_i) + b_m \quad (14)$$

Where  $W_{mj}$  is the weight between the hidden neuron  $j$  and the output neuron  $m$ ,  $W_{ji}$  is the weight between the hidden neuron  $j$  and the input neuron  $i$ ,  $X_i$  is the input value, and  $b_i$  and  $b_m$  are biases for the hidden layer and output layer, respectively. For the  $m^{th}$  network output, the derivative (PD) of output is differentiated concerning  $i^{th}$  input (“Eq. 15”).

$$\frac{\partial y_m}{\partial x_i} = \sum_j W_{jk} \left( 1 - (\sum_i W_{ji} X_i + b_i)^2 \right) W_{ji} \quad (15)$$

For N observations, there are N partial derivatives and they will be calculated for each input parameter. Thus, the relative contribution (“Eq. 16”) of each input is calculated using the total value of the squares of partial derivatives (SSD) [41–42].

$$SSD_i = \sum_{p=1}^N \left( \frac{\partial y_m}{\partial x_i} \right)_p^2 \quad (16)$$

Where  $\left( \frac{\partial y_m}{\partial x_i} \right)$  is the Pad for  $p^{th}$  observation.

Finally, the contribution for each input parameter is calculated using (“Eq. 17”):

$$\text{Contribution for } p^{th} \text{ variable} = \frac{SSD_i}{\sum SSD_i} \times 100\% \quad (17)$$

It is obvious that the parameter with the highest SSD will affect the output most significantly. Therefore, the input parameters can be sorted based on the order of SSD values, showing the relative importance of each input parameter on output. “Table. 5” shows the sensitivity analysis of the developed model input parameters on average grain size.

**Table 5** The sensitivity analysis for average grain size

No	Variables	SSD	Contribution (%)	Rank
1	RS	31.5634034	73.27699	1
2	VS	7.4543113	17.30578606	2
3	HS	4.0563835	9.417222	3

## 11 CONCLUSIONS

In this work, magnesium chips have been recycled through friction stir extrusion and the average grain size have been used as a metric to investigate the wires' quality. Choosing average grain size as an output and rotational speed, vertical speed, and extrusion hole size as the input of the system, the artificial neural network is used to model the process. Comparing different architecture, the best performance is achieved by 3–6–1 architecture which has “Tansig” and “Purelin” transfer function for hidden and the output layer with the back-propagation rate. The equation for calculating average grain size has been extracted based on the developed neural network to predict the output as a function of rotational speed, vertical speed, and extrusion hole size.

The developed model correlation coefficient and the Root–Mean–Square–Error (RMSE) (0.94438 and 0.75794, respectively) have shown that the predicted and experimental results are in good agreement. Finally, a sensitivity analysis has been conducted on the ANN model to determine the impact of each input parameter on the average grain size. Considering Pad method as a more reliable technique, the rotational speed has more effect on average grain size during the FSE process in comparison to other input parameters.

## 12 APPENDIX

The weights between of hidden layer and input and output layer are shown in “Table 6”. To calculate the relative importance of each input parameters, firstly, the absolute value of output layer weight multiplies by each hidden layer weight value ( $P_{ik}$ ) that is presented in “Table 7”. Then, for obtaining the  $Q_{ik}$ ,  $P_{ik}$  is divided into the sum value of each neuron which is shown in “Table 8”. For example, for the first input parameter and first neuron, we have:  $Q_{11} = P_{11}/P_{11} + P_{12} + P_{13}$ . Finally, for all of the input parameters,  $S_i$  is calculated by  $Q_{ik}$  summation. As an example, for first input parameter it is as following:  $S_1 = Q_{11} + Q_{21} + Q_{31} + Q_{41} + Q_{51} + Q_{61}$ . Therefore, by dividing  $S_i$  into the sum value of S, the relative importance of each input parameters can be calculated separately. For instance, the relative importance of the rotational speed is calculated as:  $(S_1 * 100) / (S_1 + S_2 + S_3)$ .

**Table 6** Different layers weights

Hidden layer neuron No.	Weight of different layer			
	Rotational Speed	Vertical Speed	Hole Size	Grain Size
1	1.47266	1.00608	-1.93075	-0.62244
2	1.72452	1.360273	0.321748	0.382324
3	-2.25114	0.57049	0.783208	-0.79684
4	-0.71733	0.256621	-2.99931	-0.29625
5	0.019349	-1.11877	1.992122	-0.33067
6	2.827377	0.117701	-0.04241	-0.98962

**Table 7** The  $P_{ik}$  calculation of different input parameters

Hidden layer neuron No.	Rotational Speed	Vertical Speed	Hole Size	Sum
1	$P_{11}=0.916642$	$P_{12}=0.922216$	$P_{13}=1.201776$	3.040634
2	$P_{21}=0.659325$	$P_{22}=0.896863$	$P_{23}=0.123012$	1.6792
3	$P_{31}=1.793798$	$P_{32}=1.023344$	$P_{33}=0.624091$	3.441234
4	$P_{41}=0.212509$	$P_{42}=0.054534$	$P_{43}=0.888546$	1.155589
5	$P_{51}=0.006398$	$P_{52}=0.007158$	$P_{53}=0.658735$	0.672291
6	$P_{61}=2.798029$	$P_{62}=0.329331$	$P_{63}=0.04197$	3.169329

Table 8 The  $Q_{ik}$  Calculation of different input parameters

Hidden layer neuron No.	Rotational Speed	Vertical Speed	Hole Size
1	$Q_{11}=0.301464$	$Q_{12}=0.303297$	$Q_{13}=0.395239$
2	$Q_{21}=0.392643$	$Q_{22}=0.534101$	$Q_{23}=0.073256$
3	$Q_{31}=0.521266$	$Q_{32}=0.297377$	$Q_{33}=0.181357$
4	$Q_{41}=0.183897$	$Q_{42}=0.047192$	$Q_{43}=0.768912$
5	$Q_{51}=0.009517$	$Q_{52}=0.010647$	$Q_{53}=0.979836$
6	$Q_{61}=0.882846$	$Q_{62}=0.103912$	$Q_{63}=0.013242$
Sum Value	$S_1=2.291632$	$S_2=1.296526$	$S_3=2.411842$

## REFERENCES

- [1] Zhang, T., Ji, Z., and Wu, S., Effect of Extrusion Ratio on Mechanical and Corrosion Properties of AZ31B Alloys Prepared by a Solid Recycling Process, *Materials and Design*, Vol. 32, No. 5, 2011, pp. 2742–2748.
- [2] Ansari, M. A., Behnagh, R. A., Narvan, M., Naeini, E. S., Givi, M. K. B., and Ding, H., Optimization of Friction Stir Extrusion (FSE) Parameters Through Taguchi Technique, *Transaction of Indian Institute of Metals*, Vol. 69, No. 7, 2016, pp. 1351–1357.
- [3] Sharifzadeh, M., Ansari, M. A., Narvan, M., Behnagh, R. A., Araee, A., and Besharati Givi, M. K., Evaluation of Wear and Corrosion Resistance of Pure Mg Wire Produced by Friction Stir Extrusion, *Transaction of Nonferrous Metals Society of China*, Vol. 25, No. 6, 2015, pp. 1847–1855.
- [4] Ji, Z. S., Wen, L. H., and Li, X. L., Mechanical Properties and Fracture Behavior of Mg–2.4Nd–0.6Zn–0.6Zr Alloys Fabricated by Solid Recycling Process, *Journal of Materials Processing Technology*, Vol. 209, No. 4, 2009, pp. 2128–2134.
- [5] Hu, M. L., Ji, Z. S., Chen, X. Y., Wang, Q. D., and Ding, W. J., Solid-State Recycling of AZ91D Magnesium Alloy Chips, *Transaction of Nonferrous Metals Society of China*, Vol. 22, No. 1, 2012, pp.68-73.
- [6] Chino, Y., Kishihara, R., Shimojima, K., Hosokawa, H., Yamada, Y., Wen, C., Iwasaki, H., and Mabuchi, M., Superplasticity and Cavitation of Recycled AZ31 Magnesium Alloy Fabricated by Solid Recycling Process, *Mater. Trans.*, Vol. 43, No. 10, 2002, pp. 2437–2442.
- [7] Wen, L., Ji, Z., and Li, X., Effect of Extrusion Ratio on Microstructure and Mechanical Properties of Mg–Nd–Zn–Zr Alloys Prepared by a Solid Recycling Process, *Materials Characterization*, Vol. 59, No. 11, 2008, pp. 1655–1660.
- [8] Tang, W., Reynolds, A. P., Production of Wire via Friction Extrusion of Aluminum Alloy Machining Chips, *Journal of Materials Processing Technology*, Vol. 210, No. 15, 2010, pp. 2231–2237.
- [9] Nicholas, E. D., Friction Processing Technologies, *Advanced Materials & Processes*, Vol. 155, No. 6, 1999, pp. 69–71.
- [10] Fehrenbacher, A., Schmale, J. R., Zinn, M. R., and Pfefferkorn, F. E., Measurement of Tool-Workpiece Interface Temperature Distribution in Friction Stir Welding, *Journal of Manufacturing Science Engineering*, Vol. 136, No. 2, 2014, pp. 021009.
- [11] Pellegrino, J. L., Margolis, N., Justiniano, M., Miller, M., and Thedki, A., Energy Use, Loss and Opportunities Analysis: US Manufacturing and Mining, DOE/ITP (U.S. Dep. Energy’s Industrial Technol. Program), (December), 2004, pp. 169.
- [12] Das, S. K., Green, J. A. S., Kaufman, J. G., Emadi, D., and Mahfoud, M., Aluminum Recycling-An Integrated, Industrywide Approach, *The Journal of The Minerals, Metals & Materials Society*, Vol. 62, No. 2, 2010, pp. 23–26.
- [13] Ansari, M. A., Sadeqzadeh Naeini, E., Besharati Givi, M. K., and Faraji, G., Theoretical and Experimental Investigation of the Effective Parameters on the Microstructure of Magnesium Wire Produced by Friction Stir Extrusion, Vol. 15, No. 6, 2015, pp. 346–352.
- [14] Huang, W., Hou, B., Pang, Y., and Zhou, Z., Fretting Wear Behavior of AZ91D and AM60B Magnesium Alloys, *Wear*, Vol. 260, No. 11–12, 2006, pp. 1173–1178.
- [15] Kang, S., Lee, Y., and Lee, J., Effect of Grain Refinement of Magnesium Alloy AZ31 by Severe Plastic Deformation on Material Characteristics, *Journal of Materials Processing Technology*, Vol. 201, No. 1–3, 2008, pp. 436–440.
- [16] Behnagh, R. A., Shen, N., Ansari, M. A., Narvan, M., Besharati Givi, M. K., and Ding, H., Experimental Analysis and Microstructure Modeling of Friction Stir Extrusion of Magnesium Chips, *Journal of Manufacturing Science and Engineering*, Vol. 138, No. 4, 2015, pp. 041008.
- [17] Grum, J., Slabe, J. M., The Use of Factorial Design and Response Surface Methodology for Fast Determination of Optimal Heat Treatment Conditions of Different Ni–Co–Mo Surfaced Layers, *Journal of Materials Processing Technology*, Vol. 155–156, 2004, pp. 2026–2032.
- [18] Lakshminarayanan, A. K., Balasubramanian, V., Comparison of RSM with ANN in Predicting Tensile Strength of Friction Stir Welded AA7039 Aluminium Alloy Joints, *Transactions of Nonferrous Metals Society of China*, Vol. 19, No. 1, 2009, pp. 9–18.
- [19] Elatharasan, G., Kumar, V. S. S., An Experimental Analysis and Optimization of Process Parameter on

- Friction Stir Welding of AA 6061-T6 Aluminum Alloy Using RSM, *Procedia Engineering*, Vol. 64, 2013, pp. 1227–1234.
- [20] Palanivel, R., KoshyMathews, P., and Murugan, N., Development of Mathematical Model to Predict the Mechanical Properties of Friction Stir Welded AA6351 Aluminum Alloy, *Journal of Engineering Science and Technology*, Vol. 4, No. 1, 2011, pp. 25–31.
- [21] Rajakumar, S., Muralidharan, C., and Balasubramanian, V., Establishing Empirical Relationships to Predict Grain Size and Tensile Strength of Friction Stir Welded AA 6061-T6 Aluminium Alloy Joints, *Transaction of Nonferrous Metals Society of China*, Vol. 20, No. 10, 2010, pp. 1863–1872.
- [22] Elangovan, K., Balasubramanian, V., and Babu, S., Predicting Tensile Strength of Friction Stir Welded AA6061 Aluminium Alloy Joints by a Mathematical Model, *Materials and Design*, Vol. 30, No. 1, 2009, pp. 188–193.
- [23] Okuyucu, H., Kurt, A., and Arcaklioglu, E., Artificial Neural Network Application to the Friction Stir Welding of Aluminum Plates, *Materials and Design*, Vol. 28, No. 1, 2007, pp. 78–84.
- [24] Asadi, P., Givi, M. K. B., Rastgoo, A., Akbari, M., Zakeri, V., and Rasouli, S., Predicting the Grain Size and Hardness of AZ91/SiC Nanocomposite by Artificial Neural Networks, *International Journal of Advanced Manufacturing Technology*, Vol. 63, No. 9-12, 2012, pp. 1095–1107.
- [25] Yousif, Y. K., Daws, K. M., and Kazem, B. I., Prediction of Friction Stir Welding Characteristic Using Neural Network, *JJMIE Jordan J. Mech. Ind. Eng.*, Vol. 2, No. 3, 2008, pp. 151–155.
- [26] Ghetiya, N. D., Patel, K. M., Prediction of Tensile Strength in Friction Stir Welded Aluminium Alloy Using Artificial Neural Network, *Procedia Technology*, Vol. 14, 2014, pp. 274–281.
- [27] Arunchai, T., Sonthipermpon, K., Apichayakul, P., and Tamee, K., Resistance Spot Welding Optimization Based on Artificial Neural Network, Vol. 2014, 2014, pp.1-6.
- [28] Bourquin, J., Schmidli, H., Van Hoogevest, P., and Leuenberger, H., Advantages of Artificial Neural Networks (ANNs) as Alternative Modelling Technique for Data Sets Showing Non-Linear Relationships Using Data from a Galenical Study on a Solid Dosage Form, *European Journal of Pharmaceutical Sciences*, Vol. 7, No. 1, 1998, pp. 5–16.
- [29] Li, H. J., Qi, L. H., Han, H. M., and Guo, L. J., Neural Network Modeling and Optimization of Semi-Solid Extrusion for Aluminum Matrix Composites, *Journal of Materials Processing Technology*, Vol. 151, 2004, pp. 126–132.
- [30] Ates, H., Prediction of Gas Metal Arc Welding Parameters Based on Artificial Neural Networks, *Materials and Design*, Vol. 28, No. 7, 2007, pp. 2015–2023.
- [31] Muthukrishnan, N., Davim, J. P., Optimization of Machining Parameters of Al/SiC-MMC with ANOVA and ANN Analysis, *Journal of Materials Processing Technology*, Vol. 209, No. 1, 2009, pp. 225–232.
- [32] Demuth, H., Beale, M., *Neural Network Toolbox For Use with MATLAB*, 1992, Aerospace, p. 846.
- [33] Kumar, P., Nigam, S. P., and Kumar, N., Vehicular Traffic Noise Modeling Using Artificial Neural Network Approach, *Transportation Research Part C*, Vol. 40, 2014, pp. 111–122.
- [34] Ferreira, P., Ribeiro, P., Antunes, A., and Dias, F. M., A High Bit Resolution FPGA Implementation of a FNN with a New Algorithm for the Activation Function, *Neurocomputing*, Vol. 71, No. 1–3, 2007, pp. 71–77.
- [35] Tuntas, R., Dikici, B., An Investigation on the Aging Responses and Corrosion Behaviour of A356/SiC Composites by Neural Network: The Effect of Cold Working Ratio, *Journal of Composite Materials*, Vol. 50, No. 17, 2016, pp. 2323–2335.
- [36] Montano, J., Palmer, A., Numeric Sensitivity Analysis Applied to Feedforward Neural Networks, *Neural Computing and Applications*, Vol. 12, No. 2, 2003, pp. 119–125.
- [37] Campana, R. C., Vieira, P. C., and Plaut, R. L., Aplicability of Adaptive Neural Networks (Ann) in the Extrusion of Aluminum Alloys and in the Prediction of Hardness and Internal Defects, *Materials Science Forum*, Vol. 638-642, 2010, pp. 303–309.
- [38] Song, R., Zhang, Q., Tseng, M., and Zhang, B., The Application of Artificial Neural Networks to the Investigation of Aging Dynamics in 7175 Aluminium Alloys, *Materials Science and Engineering C*, Vol. 3, 1995, pp. 7–9.
- [39] Garson, G. D., Interpreting Neural Network Connection Weights, *AI Expert*, Vol. 6, No. 4, 1991, pp. 46–51.
- [40] Wang, W., Jones, P., and Partridge, D., Assessing the Impact of Input Features in a Feedforward Neural Network, *Neural Computing and Applications*, Vol. 9, No. 2, 2000, pp. 101–112.
- [41] Dutta, S., Gupta, J. P., PVT Correlations for Indian Crude Using Artificial Neural Networks, *Journal of Petroleum Science and Engineering*, Vol. 72, No. 1–2, 2010, pp. 93–109.
- [42] Gevrey, M., Dimopoulos, I., and Lek, S., Review and Comparison of Methods to Study the Contribution of Variables in Artificial Neural Network Models, *Ecological Modelling*, Vol. 160, 2003, pp. 249–264.